Int. J. Heat Mass Transfer. Vol. 35, No. 12, pp. 3375–3387, 1992
Printed in Great Britain

0017–9310/92 $5.00 + 0.00

A near-wall two-equation model for turbulent heat fluxes

T. P. SOMMER, R. M. C. SO and Y. G. LAI†
Mechanical and Aerospace Engineering, Arizona State University, Tempe, AZ 85287-6106, U.S.A.

(*Received* 14 *September* 1991 *and in final form* 15 *January* 1992)

Abstract—A near-wall two-equation model for turbulent heat fluxes is derived from the temperature variance and its dissipation-rate equations and the assumption of gradient transport. Only incompressible flows with non-buoyant heat transfer are considered. The near-wall asymptotics of each term in the exact equations are examined and used to derive near-wall correction functions that render the modeled equations consistent with these behavior. Thus modeled, the equations are used to calculate fully-developed pipe and channel flows with heat transfer. It is found that the proposed two-equation model yields asymptotically correct near-wall behavior for the normal heat flux, the temperature variance and its near-wall budget and correct limiting wall values for these properties compared to direct simulation data and measurements obtained under different wall boundary conditions.

INTRODUCTION

IN THE past, turbulent flow calculations were performed using wall functions to describe the flow between the first grid point and the wall. This was necessary because the modeled equations were valid for high-Reynolds-number flows only and, therefore, could not be applied at and near a wall. The wall functions were derived assuming Couette flow and local equilibrium turbulence. These assumptions were later found to be not quite valid even for simple wall shear flows with and without heat transfer, such as fully-developed channel and pipe flows and flat plate boundary-layer flows [1–10].

The need to modify wall functions and to render the modeled turbulence equations valid at and near a wall was recognized long before direct simulation data on channel flows [1–6] were available. This recognition led to the development of near-wall or low-Reynolds-number models for two-equation and Reynolds-stress closures. Near-wall corrections were proposed and they were usually in the form of extra terms added to the turbulent kinetic energy and its dissipation rate equations [11, 12] and to the Reynolds-stress equation [13, 14]. These extra terms were derived to render the modeled equations valid at the wall and little consideration was given to ensure correct near-wall asymptotic behavior as in the exact equations. With the availability of direct simulation data [1–3], turbulence statistics near a wall and their limiting wall values can be determined accurately. As a result, most of the added functions were found to give incorrect turbulence properties near a wall [15, 16]. In particular, they failed to yield correct predictions of the limiting values of the turbulence statistics at the wall and were not able to give an asymptotic near-wall behavior similar to that given by direct numerical simulation. Recent near-wall proposals remedied some of these drawbacks. Consequently, fairly correct asymptotic near-wall modifications for two-equation [15, 17] and Reynolds-stress models [16, 18–20] are now available. These recent near-wall models have been analysed and compared with direct simulation data. Some of them are found to yield results that are in good agreement with simulation data at fairly low Reynolds numbers and with measurements at relatively high Reynolds numbers [15, 16].

In heat transfer modeling, especially incompressible non-buoyant flows, the assumption of a constant turbulent Prandtl number is usually invoked. In other words, turbulent heat fluxes were directly determined from turbulent momentum fluxes, and there was no need to solve equations that governed the transport of heat fluxes or temperature variance and its dissipation rate depending on whether the assumption of gradient transport was made. It was further argued that better predictions of near-wall turbulent heat fluxes and their asymptotic behavior could be achieved by improving near-wall models for the velocity field [21, 22]. However, recent shear flow measurements [7–10] and direct simulation data [4–6] showed that an analogy between heat and momentum transfer as represented by a constant turbulent Prandtl number could not adequately reflect the physical phenomenon of heat transport, even for simple wall shear flows. Furthermore, these data showed that the turbulent Prandtl number, instead of being constant, increased towards a wall. Its value at the wall was determined to be about 1.1 and far exceeded the 0.7–0.9 value normally assumed for wall shear flow calculations. In other words, if turbulent heat transfer were to be

† Presently at CFD Research Corp., Huntsville, AL 35802, U.S.A.

NOMENCLATURE

A^+ model constant, taken to be 30

a_i, b_i, c_i, d_i random functions of time and the x and z coordinates

a_{uv}, b_{uv} coefficients in the expansion for $\overline{uv}^+$ in the near-wall region

a_θ, b_θ coefficients in the expansion for θ^{+2} in the near-wall region

$a_{u\theta}$, $b_{u\theta}$ coefficients in the expansion for $\overline{u\theta}^+$ in the near-wall region

$a_{v\theta}$, $b_{v\theta}$ coefficients in the expansion for $\overline{v\theta}^+$ in the near-wall region

$a_{\varepsilon\theta}$, $b_{\varepsilon\theta}$ coefficients in the expansion for ε_θ^+ in the near-wall region

A, B, C, D coefficients in the expansion for $\overline{\theta^2}$ and ε_θ

c_1 model constant, taken to be 1.5

c_2 model constant, taken to be 0.4

c_s model constant, taken to be 0.11

c_ε model constant, taken to be 0.15

$c_{\varepsilon 1}$ model constant, taken to be 1.35

$c_{\varepsilon 2}$ model constant, taken to be 1.8

C_p specific heat at constant pressure

$C_{1\lambda}$ model constant, taken to be 0.1

C_{d1} model constant, taken to be 1.8

C_{d2} model constant, taken to be zero

C_{d3} model constant, taken to be 0.72

C_{d4} model constant, taken to be 2.2

C_{d5} model constant, taken to be 0.8

C_λ model constant, taken to be 0.11

C_{θ^2} model constant, taken to be 0.11

$C_{\varepsilon\theta}$ model constant, taken to be 0.11

D_θ^* molecular diffusion term in temperature variance equation

$D_{\varepsilon\theta}^*$ molecular diffusion term in ε_θ equation

$D_{\varepsilon\theta}^t$ turbulent diffusion term in ε_θ equation

$f_{w,1}$ near-wall damping function for Reynolds-stress equation

$f_{w,2}$ near-wall damping function for ε equation

$f_{w,\varepsilon\theta}$ near-wall damping function for ε_θ equation

f_λ near-wall damping function for turbulent heat diffusivity

f_ε near-wall damping function for ε equation

h channel half width

k turbulent kinetic energy

n_i unit normal vector measured positive outward from wall

$\tilde{P}$ production due to mean shear, $-u_iu_j(\partial U_i/\partial x_j)$

P_θ production due to mean temperature, $-\overline{u_k\theta}(\partial\Theta/\partial x_k)$

$P_{\varepsilon\theta}$ production term in the ε_θ equation

P_θ^* production term due to mean temperature gradient in the x-direction

Pr molecular Prandtl number

Pr_t turbulent Prandtl number

q_w wall heat flux

R time scale ratio

Re Reynolds number based on mean bulk velocity, $U_0(2h)/\nu$

Re_τ Reynolds number based on the wall friction velocity, $u_\tau h/\nu$

Re_t turbulent Reynolds number, $k^2/\nu\varepsilon$

S_θ source term in temperature variance and its dissipation rate equations

t time

U_0 mean bulk velocity

U, V mean velocity components along x and y, respectively

U_i ith component of the mean velocity

U^+ normalized mean U velocity, U/u_τ

u_i ith component of the fluctuating velocity

u, v, w fluctuating velocity components along x, y and z, respectively

u_τ friction velocity, $(\tau_w/\rho)^{1/2}$

$\overline{uv}^+$ normalized turbulent shear stress, $\overline{uv}/u_\tau^2$

$\overline{v\theta}^+$ normalized turbulent heat flux, $\overline{v\theta}/u_\tau\Theta_\tau$

$\overline{u\theta}^+$ normalized turbulent heat flux, $\overline{u\theta}/u_\tau\Theta_\tau$

x_i ith component of the coordinate

x, y, z coordinates along stream, normal and transverse directions

y^+ normalized y coordinate, yu_τ/ν.

Greek symbols

α thermal diffusivity, $\kappa_t/\rho C_p$

α_t turbulent heat diffusivity

α^* model constant, taken to be 0.45

ε solenoidal dissipation rate of k

ε_θ dissipation rate of temperature variance

$\tilde{\varepsilon}$ dissipation rate, $\varepsilon - 2\nu(\partial\sqrt{k}/\partial y)^2$

$\tilde{\varepsilon}_\theta$ dissipation rate, $\varepsilon_\theta - \alpha(\partial\sqrt{\overline{\theta^2}}/\partial y)^2$

ε^* dissipation rate, $\varepsilon - 2\nu k/y^2$

ε_θ^* dissipation rate, $\varepsilon_\theta - \alpha\overline{\theta^2}/y^2$

ε^+ normalized dissipation rate, $\varepsilon\nu/u_\tau^4$

ε_θ^+ normalized dissipation rate, $\varepsilon_\theta\nu/u_\tau^2\Theta_\tau^2$

Θ mean temperature

Θ_τ friction temperature, $q_w/\rho C_p u_\tau$

Θ^+ normalized mean temperature, Θ/Θ_τ

θ fluctuating temperature

$\overline{\theta^2}$ temperature variance

θ_{rms}^+ normalized rms temperature variance, $\sqrt{\overline{\theta^2}}/\Theta_\tau$

κ_t thermal conductivity

κ von Karman constant for the velocity profile

κ_θ von Karman constant for the temperature profile

ν fluid kinematic viscosity

ξ near-wall correction to ε equation

$\xi_{\varepsilon\theta}$ near-wall correction to ε_θ equation

ρ instantaneous fluid density

$\Sigma_{\varepsilon\theta}$ dissipation term in ε_θ equation

τ_w wall shear stress.

Overbars

$\overline{}$ time-averaged quantities.

calculated correctly in non-buoyant wall shear flows, the constant turbulent Prandtl number assumption has to be relaxed.

For incompressible non-buoyant flows, the exact mean momentum equations are decoupled from the mean energy equation and the exact transport equations for the turbulent heat fluxes do not contain a temperature variance term. Therefore, they can be solved without knowledge of the temperature variance if a second-order closure for the heat fluxes [23] is used. In other words, the mean temperature distributions can be calculated independent of the temperature variance and its dissipation rate. Furthermore, the velocity field is not affected by the temperature field and momentum fluxes can be modeled independent of heat fluxes. Consequently, two independent approaches can be proposed for the modeling of near-wall heat transport in such flows. One approach is to invoke gradient transport for the heat fluxes and then relate them to temperature variance and its dissipation rate in a manner similar to that used to define turbulent eddy viscosity. Therefore, this necessitates near-wall modeling of temperature variance and its dissipation rate equations. Such a model has been proposed by Nagano and Kim [21] and their predictions of mean flow properties are in good agreement with measurements. However, in their model, they assumed the dissipation rate of temperature variance to be zero at the wall. This assumption is not consistent with measurements and direct simulation data [4–6, 10].

Another approach is to model and solve the heat flux equations, thus avoiding the assumption of a vanishing dissipation rate of the temperature variance at the wall. An asymptotically correct heat flux model has been derived by Lai and So [23] using the approach proposed in ref. [20]. Consequently, the modeled heat flux equations yield an asymptotic behavior correct to first order compared to the exact equations. The calculated normal heat flux is in excellent agreement with measurements [8] and the turbulent Prandtl number is predicted to vary across the pipe and to increase as the wall is approached. On the other hand, for buoyant flows, the transport equations for the heat fluxes contain a temperature variance term. In this case, equations for the temperature variance and its dissipation rate need to be solved, even if a second-order closure for the heat fluxes is used. Therefore, if near-wall heat transfer were to be calculated accurately for non-buoyant and buoyant flows, an asymptotically correct near-wall model has to be derived for the temperature variance and its dissipation rate equations.

The present objective is to derive and validate an asymptotically correct near-wall two-equation model for heat transport based on the temperature variance and its dissipation rate equations. This is accomplished by analyzing the near-wall behavior of the terms in the exact equations. A conventional high-Reynolds-number model for these equations is chosen and its behavior near a wall is examined. Near-wall modifications to the high-Reynolds-number models are proposed to remedy the differences between the exact and modeled behavior of the terms in the near-wall region. Obviously, a complete remedy cannot be expected. Instead, the modifications are derived to match the behavior up to first order of the coordinate normal to the wall.

For the type of flow under consideration, the velocity field is not influenced by the temperature field. Theoretically, therefore, any closure model for the momentum fluxes can be used to calculate the velocity field. In order to ensure accuracy and reliability in the calculated velocity field, it is prudent to select a higher-order model for the momentum fluxes. Therefore, a second-order near-wall model for the momentum fluxes and the proposed two-equation model for heat fluxes is used to calculate fully-developed pipe and channel flows with different wall thermal boundary conditions. The calculations are validated against measurements and direct simulation data and the results are also compared with the model predictions of refs. [21, 23].

TEMPERATURE VARIANCE AND ITS DISSIPATION RATE EQUATIONS

If temperature variance is denoted by $\overline{\theta^2}$ and its dissipation rate ε_θ is defined as

$$\varepsilon_\theta = \alpha \overline{\frac{\partial \theta}{\partial x_k}\frac{\partial \theta}{\partial x_k}} \tag{1}$$

then the exact equations governing the transport of $\overline{\theta^2}$ and ε_θ are given by [24]

$$\frac{\partial \overline{\theta^2}}{\partial t} + \frac{\partial}{\partial x_k}(U_k\overline{\theta^2}) = \frac{\partial}{\partial x_k}\left(\alpha\frac{\partial \overline{\theta^2}}{\partial x_k}\right) - \frac{\partial}{\partial x_k}(\overline{u_k\theta^2}) - 2\overline{u_k\theta}\frac{\partial \Theta}{\partial x_k} - 2\alpha\overline{\frac{\partial \theta}{\partial x_k}\frac{\partial \theta}{\partial x_k}} + 2\overline{\theta S_\theta} \tag{2}$$

$$\frac{\partial \varepsilon_\theta}{\partial t} + \frac{\partial}{\partial x_k}(U_k\varepsilon_\theta) = \frac{\partial}{\partial x_k}\left(\alpha\frac{\partial \varepsilon_\theta}{\partial x_k}\right) - \frac{\partial}{\partial x_k}(\overline{u_k\varepsilon_\theta}) - 2\alpha\overline{\frac{\partial \theta}{\partial x_j}\frac{\partial u_k}{\partial x_j}\frac{\partial \Theta}{\partial x_k}} - 2\alpha\overline{u_k\frac{\partial \theta}{\partial x_j}\frac{\partial^2 \Theta}{\partial x_k\,\partial x_j}} - 2\alpha\overline{\frac{\partial \theta}{\partial x_j}\frac{\partial \theta}{\partial x_k}\frac{\partial U_k}{\partial x_j}} - 2\alpha\overline{\frac{\partial \theta}{\partial x_j}\frac{\partial u_k}{\partial x_j}\frac{\partial \theta}{\partial x_k}} - 2\overline{\left(\alpha\frac{\partial^2 \theta}{\partial x_k\,\partial x_j}\right)^2} + 2\alpha\overline{\frac{\partial \theta}{\partial x_j}\frac{\partial S_\theta}{\partial x_j}}. \tag{3}$$

In equations (2) and (3), S_θ is a source term involving fluctuating viscous stresses and fluctuating velocity gradients.

It is clear from the exact transport equations (2) and (3) that the relative importance of the different terms in the $\overline{\theta^2}$ and ε_θ budgets is similar to that of the corresponding terms in the equations governing the transport of turbulent kinetic energy (k) and its dissipation rate (ε). Several experimental studies have shown that close similarity does exist between the budgets of k and ε and $\overline{\theta^2}$ and ε_θ. For example, the

boundary-layer measurements of Krishnamoorthy and Antonia [9, 10] indicated that the thermal and velocity fields resemble each other. Particularly, the measurements of ε_θ have enabled the temperature dissipation time scale to be estimated in the near-wall region and approximately the same distribution as the velocity dissipation time scale was obtained. In view of this and the assumption of incompressible flow, the last term in (2) and (3) is small compared to other terms and can be neglected. Therefore, in the following, their modeling need not be discussed.

Most proposals for turbulent diffusion modeling in the $\overline{\theta^2}$ equation have adopted a gradient-type representation for $\overline{u_k\theta^2}$. Consistent with conventional approaches and with diffusion modeling of the velocity field [20], the following model is suggested, or

$$-\overline{u_k\theta^2} = C_{\theta^2}\overline{u_k u_j}\frac{k}{\varepsilon}\frac{\partial\overline{\theta^2}}{\partial x_j}. \tag{4}$$

The diffusion coefficient C_{θ^2} is chosen to be 0.11 as recommended by Launder [24]. This proposal can be adopted for both low- and high-Reynolds-number flows, the reason being that an asymptotic analysis of (2) reveals that turbulent diffusion of $\overline{\theta^2}$ is at most of order y^3 near a wall and, therefore, is negligible compared to dissipation and molecular diffusion of $\overline{\theta^2}$. Furthermore, experimental measurements [9, 10] support this assumption. Also, since the modeled term (4) is of higher order, it has little or no effect on the near-wall analysis of (2).

A more important term requiring approximation in the $\overline{\theta^2}$ equation is the dissipation rate ε_θ. In most previous studies, this dissipation rate is algebraically related to $\overline{\theta^2}$ through the use of a time-scale ratio R [24, 25] that has a range of 0.5–0.8 depending on the flow problem considered. Unfortunately, measurements of the decay of temperature and velocity fluctuations behind a heated grid suggest that the time-scale ratio has a rather wide scatter and is not sufficiently constant to serve as a general method for the determination of ε_θ. The alternative is to determine ε_θ from its own transport equation, which is given by (3).

The problem of closing (3) is much more difficult than that of the ε equation because there are more time and generation-rate scales in the ε_θ equation. For high-Reynolds-number flows, dimensional analysis suggests that only the sixth and seventh terms on the right hand side of (3) are important. Several proposals have been made to close the ε_θ equation for high-Reynolds-number flows [21, 26–29]. Among them, the proposal of Jones and Musonge [26] takes the form:

$$\frac{D\varepsilon_\theta}{Dt} = D^t_{\varepsilon\theta} + P_{\varepsilon\theta} - \Sigma_{\varepsilon\theta} \tag{5}$$

where

$$P_{\varepsilon\theta} = C_{d2}\frac{\varepsilon}{k}P_\theta + C_{d3}\varepsilon_\theta\frac{\tilde{P}}{k} \tag{6}$$

$$\Sigma_{\varepsilon\theta} = C_{d4}\frac{\varepsilon_\theta}{\overline{\theta^2}}\varepsilon_\theta + C_{d5}\frac{\varepsilon}{k}\varepsilon_\theta. \tag{7}$$

Note that in the modeling of $P_{\varepsilon\theta}$ and $\Sigma_{\varepsilon\theta}$, terms involving the generation and destruction of fine scale turbulence interactions, both thermal and velocity time scales are used. However, in the second-order closures of Newman *et al.* [27] and Elghobashi and Launder [28], only the thermal time scale and the thermal production rate are used to model $P_{\varepsilon\theta}$. On the other hand, Nagano and Kim [21] propose to use both production rates to model $P_{\varepsilon\theta}$, or

$$P_{\varepsilon\theta} = C_{d1}\frac{\varepsilon_\theta}{\overline{\theta^2}}P_\theta + C_{d3}\varepsilon_\theta\frac{\tilde{P}}{k}. \tag{8}$$

It is worth noting that recently, Yoshizawa [29] was able to derive the same form as (7) and (8) for the models for $\Sigma_{\varepsilon\theta}$ and $P_{\varepsilon\theta}$ using statistical results obtained from a two-scale direct-interaction approximation. Even the model constants predicted by their direct-interaction approximation are approximately the same as those proposed by Newman *et al.* [27]. Since it is generally agreed that both temperature and velocity time scales and production rates affect ε_θ, it would seem that a more general form for $P_{\varepsilon\theta}$ would be

$$P_{\varepsilon\theta} = C_{d1}\frac{\varepsilon_\theta}{\overline{\theta^2}}P_\theta + C_{d2}\frac{\varepsilon}{k}P_\theta + C_{d3}\varepsilon_\theta\frac{\tilde{P}}{k} \tag{9}$$

where the values of the model constants C_{d1}–C_{d3} are to be discussed later.

Finally, to close the ε_θ equation, the turbulent diffusion term, $D^t_{\varepsilon\theta}$, also needs modeling. It is proposed to model this term using a gradient-type approximation consistent with turbulent diffusion modeling in other equations. The proposed model is

$$D^t_{\varepsilon\theta} = \frac{\partial}{\partial x_k}\left(C_{\varepsilon\theta}\frac{k}{\varepsilon}\overline{u_k u_j}\frac{\partial\varepsilon_\theta}{\partial x_j}\right). \tag{10}$$

Again, the model is valid for both low- and high-Reynolds-number flows. Therefore, the modeled high-Reynolds-number $\overline{\theta^2}$ and ε_θ equations can be summarized as

$$\frac{D\overline{\theta^2}}{Dt} = \frac{\partial}{\partial x_k}\left(C_{\theta^2}\overline{u_k u_l}\frac{k}{\varepsilon}\frac{\partial\overline{\theta^2}}{\partial x_l}\right) - 2\overline{u_k\theta}\frac{\partial\Theta}{\partial x_k} - 2\varepsilon_\theta \tag{11}$$

$$\frac{D\varepsilon_\theta}{Dt} = \frac{\partial}{\partial x_k}\left(C_{\varepsilon\theta}\frac{k}{\varepsilon}\overline{u_k u_j}\frac{\partial\varepsilon_\theta}{\partial x_j}\right) + C_{d1}\frac{\varepsilon_\theta}{\overline{\theta^2}}P_\theta + C_{d2}\frac{\varepsilon}{k}P_\theta + C_{d3}\varepsilon_\theta\frac{\tilde{P}}{k} - C_{d4}\frac{\varepsilon_\theta}{\overline{\theta^2}}\varepsilon_\theta - C_{d5}\frac{\varepsilon}{k}\varepsilon_\theta. \tag{12}$$

NEAR-WALL TWO-EQUATION MODEL

The modeled equations (11) and (12) are quite general and include most proposals put forward by other researchers. Therefore, they could serve as the base model for heat transfer problems. However, these equations are not applicable at and near a wall. In order to render them valid in the near-wall region, an

extension of the above equations to low-Reynolds-number flows is required. This can be achieved in a manner analogous to the near-wall modeling of the k and ε equations [15]. First of all, the viscous diffusion terms that appeared in (2) and (3) have to be restored to (11) and (12). For incompressible flows, if the assumptions of analyticity for the turbulent fluctuations and vanishing temperature fluctuation at the wall are invoked, near-wall Taylor expansions of u_i and θ in terms of y can be written as [16, 23]:

$$u = a_1 y + a_2 y^2 + \cdots, \quad v = b_2 y^2 + \cdots, \quad \text{(13a, b)}$$

$$w = c_1 y + c_2 y^2 + \cdots, \quad \theta = d_1 y + d_2 y^2 + \cdots. \quad \text{(13c, d)}$$

While the assumption of analyticity is well accepted, (13d) is correct only for the isothermal wall boundary condition. Its extension to adiabatic and constant wall heat flux boundary conditions represents a good approximation of the fluctuating temperature behavior and is supported by the analysis of Polyakov [30]. Therefore, with the help of (13) and the addition of the viscous diffusion term to (11), it can be shown that the modeled $\overline{\theta^2}$ equation is in balance to the lowest order of y in the near-wall region and the balance is provided by viscous diffusion and viscous dissipation. This can be verified by making use of the definition of ε_θ given by (3), $k = \overline{u_i u_i}/2$ and $\varepsilon = \nu(\overline{\partial u_i/\partial x_j})^2$. In view of this, the $\overline{\theta^2}$ equation, just like its counterpart k equation, needs no further modifications for near-wall flows.

A similar near-wall asymptotic analysis of the exact and modeled ε_θ equation shows that molecular diffusion reaches a finite value at the wall and is dominant in the near-wall region. Near-wall analysis of other terms in (12) reveals that the generation terms can be of order y^0 depending on the thermal wall boundary condition assumed, while the modeled destruction terms become infinite as a wall is approached because ε and ε_θ are finite and k and $\overline{\theta^2}$ are zero at the wall. The modeled behavior is contrary to that of the exact terms. However, this singular behavior can be removed by replacing ε and ε_θ in the velocity and thermal time scales in (7) by $\tilde{\varepsilon}$ and $\tilde{\varepsilon}_\theta$. Thus modified, the near-wall behavior of the modeled ε_θ equation has the property that molecular diffusion becomes dominant when a wall is approached, while the destruction of ε_θ goes to zero at the wall. This behavior is contrary to the exact behavior dictated by (3) and is analogous to the behavior of the high-Reynolds-number form of the ε equation. Therefore, further modifications are required to effect balance of the modeled ε_θ equation in the near-wall region.

In order to achieve a proper balance of the modeled ε_θ equation in the near-wall region, a starting point of the analysis is the exact ε_θ equation. However, since the terms of the exact equation are not modeled on a one-to-one correspondence basis, an alternative condition has to be imposed to effect proper balance in the near-wall region. One such condition is that proposed by Shima [18] for the analysis of the ε equation. The present study extends this condition to analyse the ε_θ equation so that proper near-wall balance of the modeled equation is achieved. This can be accomplished by expanding the fluctuating quantities according to (13). Using the definitions of $\overline{\theta^2}$ and ε_θ and the substitution of (13), the following is obtained:

$$\overline{\theta^2} = 2Ay^2 + 2By^3 + Cy^4 + \cdots$$

$$\varepsilon_\theta = \alpha(2A + 4By + Dy^2 + \cdots) \quad \text{(14a, b)}$$

where A, B, C and D are related to the time average of the coefficients $d_1, d_2, \ldots$. Further analysis of the exact $\overline{\theta^2}$ equation at a wall yields

$$\varepsilon_\theta = \frac{\alpha}{2} \overline{\frac{\partial^2 \theta^2}{\partial x_k \partial x_k}}. \quad (15)$$

Following the proposal of Shima [18], which is formulated for the ε equation, a transport equation for the right-hand side of (15) can be derived and then approximated for near-wall flows. In order that the result is applicable for both constant wall temperature and constant wall heat flux boundary conditions, the following equation is obtained:

$$2\frac{\partial \varepsilon_\theta}{\partial t} = \frac{\partial}{\partial t}\left(\alpha \overline{\frac{\partial^2 \theta^2}{\partial x_k \partial x_k}}\right) = -2\alpha \overline{\frac{\partial^2 \varepsilon_\theta}{\partial x_k \partial x_k}} + \alpha \overline{\frac{\partial^2}{\partial x_m \partial x_m}\left(\alpha \frac{\partial^2 \theta^2}{\partial x_k \partial x_k}\right)} - 4\alpha \overline{\frac{\partial \theta}{\partial x_j}\frac{\partial u}{\partial x_j}\frac{\partial \Theta}{\partial x}}. \quad (16)$$

Another equation for $2(\partial \varepsilon_\theta/\partial t)$ can also be derived from the modeled ε_θ equation (12) with the molecular diffusion term restored and a near-wall correcting function implemented to account for low Re effect. These two equations should possess the same asymptotic behavior near a wall. Therefore, this constraint can be used to determine the near-wall correcting function, $\xi_{\varepsilon\theta}$.

Since a general analysis is difficult, the following analysis is restricted to the case where the averaged quantities are functions of y and t only. The near-wall asymptotic behavior of the right-hand side of (16) can be obtained by making use of (13) and (14). After much algebra, the result is $[-4\alpha^2 D + 24\alpha^2 C - 4\alpha \overline{a_1 d_1}(\partial\Theta/\partial x)]$. If $2(\partial \varepsilon_\theta/\partial t)$ derived from the modified modeled ε_θ equation is to give the same result to the lowest order of y, then it can be shown that the extra term $\xi_{\varepsilon\theta}$ thus deduced can be written as

$$\xi_{\varepsilon\theta} = f_{w,\varepsilon\theta}\left((C_{d4} - 4)\frac{\tilde{\varepsilon}_\theta}{\overline{\theta^2}}\varepsilon_\theta + C_{d5}\frac{\tilde{\varepsilon}}{k}\varepsilon_\theta - \frac{\varepsilon_\theta^{*2}}{\overline{\theta^2}} + (2 - C_{d1} - C_{d2}\, Pr)\frac{\varepsilon_\theta}{\overline{\theta^2}} P_\theta^*\right). \quad (17)$$

The appearance of P_θ^* in (17) is a consequence of the constant wall heat flux boundary condition, where $\partial\Theta/\partial x$ is constant. The function $f_{w,\varepsilon\theta}$ is introduced to ensure that away from the wall the contribution of $\xi_{\varepsilon\theta}$ is essentially zero. In other words, the high-Reynolds-

Table 1. A summary of the model constants proposed by various researchers

Model	C_{d1}	C_{d2}	C_{d3}	C_{d4}	C_{d5}
Nagano and Kim [21]	1.8	0	0.72	2.2	0.8
Jones and Musonge [26]	0	1.7	1.4	2.0	0.52
Newman *et al.* [27]	2.0	0	0	2.02	0.88
Elghobashi and Launder [28]	1.8	0	0	2.2	0.8
Yoshizawa [29]	1.2	0	0.52	1.2	0.52
Elghobashi and LaRue [31]	1.8	0	0.8	2.2	0.8
Present	1.8	0	0.72	2.2	0.8

number form of the equations is recovered correctly. Along the line of So *et al.*'s [15] suggestion, the following function, $f_{w,\varepsilon\theta} = \exp[-(Re_t/80)^2]$, is adopted.

In summary, the final $\overline{\theta^2}$ and ε_θ equations for near-wall flows can be modeled as:

$$\frac{D\overline{\theta^2}}{Dt} = \frac{\partial}{\partial x_k}\left(\alpha\frac{\partial\overline{\theta^2}}{\partial x_k}\right) + \frac{\partial}{\partial x_k}\left(C_s^{\theta^2}\frac{k}{\varepsilon}\overline{u_k u_j}\frac{\partial\overline{\theta^2}}{\partial x_j}\right) - 2\overline{u_k\theta}\frac{\partial\Theta}{\partial x_k} - 2\varepsilon_\theta \quad (18)$$

$$\frac{D\varepsilon_\theta}{Dt} = \frac{\partial}{\partial x_k}\left(\alpha\frac{\partial\varepsilon_\theta}{\partial x_k}\right) + \frac{\partial}{\partial x_k}\left(C_s^{\varepsilon\theta}\frac{k}{\varepsilon}\overline{u_k u_j}\frac{\partial\varepsilon_\theta}{\partial x_j}\right) + C_{d1}\frac{\varepsilon_\theta}{\overline{\theta^2}}P_\theta + C_{d2}\frac{\varepsilon}{k}P_\theta + C_{d3}\varepsilon_\theta\frac{\tilde{P}}{k} - C_{d4}\frac{\tilde{\varepsilon}_\theta}{\overline{\theta^2}}\varepsilon_\theta - C_{d5}\frac{\tilde{\varepsilon}}{k}\varepsilon_\theta + \xi_{\varepsilon\theta}. \quad (19)$$

Since $\overline{u_k\theta}$ appears in both these equations, turbulent heat fluxes also have to be modeled. Again, gradient diffusion is assumed and $-\overline{u_k\theta} = \alpha_t(\partial\Theta/\partial x_k)$ is proposed. The normal heat flux $\overline{v\theta}$ is of order y^3 near a wall according to (13) and $\partial\Theta/\partial y$ is of order y^0; therefore, the ordering of α_t has to be the same as $\overline{v\theta}$. The model suggested by Nagano and Kim [21] for α_t is

$$\alpha_t = C_\lambda f_\lambda k[k\theta^2/\varepsilon\varepsilon_\theta]^{1/2} \quad (20)$$

where $C_\lambda = 0.11$ and f_λ is a near-wall function. The function proposed by Nagano and Kim [21] does not lead to a near-wall behavior of y^3 for α_t. If this behavior is to be recovered, then f_λ has to be of order y^{-1}. In the present study, a proposal for f_λ satisfying this limiting behavior is made on the basis of Nagano and Kim's [21] suggestion, and is given by

$$f_\lambda = \left[f_{w,\varepsilon\theta}\frac{C_{1\lambda}}{\sqrt[4]{(Re_t)}}\right] + [1-\exp(-y^+/A^+)]^2 \quad (21)$$

where $C_{1\lambda}$ is taken to be 0.1 and $A^+ = 30$ as suggested in ref. [21] are constants adopted for the present study. With this proposal, equations (18) and (19) are closed and can be solved together with a near-wall model for the velocity field.

Finally, the model constants $C_{d1}, \ldots, C_{d5}$ have to be chosen. The values proposed by various researchers are summarized in Table 1. With the exception of Yoshizawa [29], most model constants are determined by considering measurements obtained in decaying homogeneous scalar turbulence and temperature variance in grid turbulence. It can be seen that, of all suggestions, the proposals of Elghobashi and Launder [28], Elghobashi and LaRue [31] and Nagano and Kim [21] are essentially identical. Since Nagano and Kim [21] have validated their constants against different types of high-Reynolds-number flows and good results are obtained, the present study adopts their proposed values.

NEAR-WALL REYNOLDS-STRESS MODEL

The mean temperature equation, together with (18) and (19), cannot be solved without knowledge of the mean velocity field and turbulent momentum fluxes. These properties can be determined by solving the mean flow equations using an appropriate closure model. Since the near-wall Reynolds-stress model of Lai and So [20] yields accurate results for wall shear flows and their channel flow calculations compare favorably with direct simulation data [1–3] and measurements [32], their model is chosen for the present calculations of heat transfer in pipe and channel flows. For the sake of completeness, the model equations are also given below.

The Reynolds-stress transport equations for incompressible turbulent flows can be symbolically written as

$$C_{ij} = D_{ij}^v + D_{ij}^t + P_{ij} + \Phi_{ij}^* - \varepsilon_{ij} \quad (22)$$

where the terms from left to right represent convection, molecular diffusion, turbulent diffusion, production by mean strain, velocity–pressure-gradient correlation and dissipation of $\overline{u_iu_j}$, respectively. In (22), only the terms D_{ij}^t, Φ_{ij}^* and ε_{ij} need modeling. Lai and So [20] use Launder *et al.*'s [33] high-Reynolds-number closure as the base model and proceed to modify it for near-wall flows. Their modifications for D_{ij}^t, Φ_{ij}^* and ε_{ij} can be written as

$$D_{ij}^t = \frac{\partial}{\partial x_k}\left\{c_s\frac{k}{\varepsilon}\left[\overline{u_iu_m}\frac{\partial\overline{u_ju_k}}{\partial x_m} + \overline{u_ju_m}\frac{\partial\overline{u_ku_i}}{\partial x_m} + \overline{u_ku_m}\frac{\partial\overline{u_iu_j}}{\partial x_m}\right]\right\} \quad (23)$$

$$\varepsilon_{ij} = \tfrac{2}{3}\varepsilon(1-f_{w,1})\delta_{ij} + f_{w,1}\frac{\varepsilon}{k}[\overline{u_iu_j} + \overline{u_iu_k}n_kn_j + \overline{u_ju_k}n_kn_i + \overline{u_ku_m}n_mn_kn_in_j]/[1+3\overline{u_ku_m}n_mn_k/2k] \quad (24)$$

$$\Phi_{ij}^* = \Phi_{ij} + \Phi_{ij,w}f_{w,1} \quad (25)$$

$$\Phi_{ij} = -c_1\frac{\varepsilon}{k}(\overline{u_iu_j} - \tfrac{2}{3}\delta_{ij}k) - \frac{(c_2+8)}{11}\left(P_{ij} - \frac{2\delta_{ij}}{3}\tilde{P}\right) - \frac{(8c_2-2)}{11}\left(D_{ij} - \frac{2\delta_{ij}}{3}\tilde{P}\right) - \frac{(30c_2-2)}{55}k\left(\frac{\partial U_i}{\partial x_j} + \frac{\partial U_j}{\partial x_i}\right) \quad (26a)$$

$$\Phi_{ij,w} = c_1\frac{\varepsilon}{k}(\overline{u_iu_j} - \tfrac{2}{3}\delta_{ij}k) - \frac{\varepsilon}{k}(\overline{u_iu_k}n_kn_j + \overline{u_ju_k}n_kn_i) + \alpha^*\left(P_{ij} - \frac{2\delta_{ij}}{3}\tilde{P}\right) \quad (26b)$$

where

$$P_{ij} = -\left\{\overline{u_i u_k}\frac{\partial U_j}{\partial x_k} + \overline{u_j u_k}\frac{\partial U_i}{\partial x_k}\right\}, \quad (27a)$$

$$D_{ij} = -\left\{\overline{u_i u_k}\frac{\partial U_k}{\partial x_j} + \overline{u_j u_k}\frac{\partial U_k}{\partial x_i}\right\} \quad (27b)$$

$f_{w,1} = \exp[-(Re_t/150)^2]$, and the model constants are given by $c_1 = 1.5$, $c_2 = 0.4$, $c_s = 0.11$ and $\alpha^* = 0.45$. These constants are the same as those specified by Launder *et al.* [33] and Lai and So [20]. The convection and molecular diffusion terms in (22) are given by $C_{ij} = \mathrm{D}\overline{u_i u_j}/\mathrm{D}t$ and $D_{ij}^{\nu} = \partial[\nu\,\partial\overline{u_i u_j}/\partial x_k]/\partial x_k$, respectively.

A transport equation valid all the way to the wall for the dissipation rate ε is required to complete closure. This equation is given by Lai and So [20] as

$$\frac{\mathrm{D}\varepsilon}{\mathrm{D}t} = \frac{\partial}{\partial x_k}\left(\nu\frac{\partial\varepsilon}{\partial x_k}\right) + \frac{\partial}{\partial x_k}\left(c_\varepsilon\frac{k}{\varepsilon}\overline{u_k u_i}\frac{\partial\varepsilon}{\partial x_i}\right) + c_{\varepsilon 1}(1+f_{w,2})\frac{\varepsilon}{k}\tilde{P} - c_{\varepsilon 2}f_\varepsilon\frac{\varepsilon\tilde{\varepsilon}}{k} + \xi \quad (28)$$

where

$$\xi = f_{w,2}\left[\left(\frac{7}{9}c_{\varepsilon 2} - 2\right)\frac{\varepsilon\tilde{\varepsilon}}{k} - \frac{1}{2}\frac{\varepsilon^{*2}}{k}\right]$$

and the model constants, specified as $c_\varepsilon = 0.15$, $c_{\varepsilon 1} = 1.35$, $c_{\varepsilon 2} = 1.8$, are taken from Launder *et al.* [33]. The damping functions are defined as $f_\varepsilon = 1-(2/9)\exp\{-(Re_t/6)^2\}$ and $f_{w,2} = \exp\{(-Re_t/64)^2\}$. It can be seen from the proposed new models for ε_{ij} and Φ_{ij}^* that as the flow moves away from a wall, $f_{w,1}$ quickly vanishes and the near-wall model of (22) reduces exactly to the high-Reynolds-number model of Launder *et al.* [33].

RESULTS AND DISCUSSION

The modeled equations (18), (19), (22) and (28) are solved with the mean momentum and temperature equations. Boundary conditions are no slip at the wall for all velocities and turbulence properties except ε which is given by $2\nu(\partial\sqrt{k}/\partial y)^2$. The thermal boundary conditions are either constant wall heat flux or constant wall temperature. As for $\overline{\theta^2}$ and ε_θ, the wall boundary conditions are $\overline{\theta^2} = 0$ and $\varepsilon_\theta = \alpha(\partial\sqrt{\overline{\theta^2}}/\partial y)^2$. The governing equations and associated boundary conditions are used to calculate heat transfer in fully-developed pipe and channel flows. Since the flow is fully developed, the equations can be reduced to ordinary differential equations and the Newton iteration scheme proposed in ref. [20] is used to numerically solve the finite difference equations. Details of this technique can be found in refs. [13, 20, 23].

Present calculations are evaluated against direct simulation data with constant wall temperature [4, 5] and with constant wall heat flux [6] boundary conditions. The former study is carried out at $Re_\tau = 180$, or $Re = 6600$, and a molecular Prandtl number $Pr = 0.71$. On the other hand, the study of Kasagi *et al.* [6] is carried out at $Re_\tau = 150$, or $Re = 4560$, and the same Pr. Since the near-wall budgets for temperature variance and its dissipation rate and for heat fluxes are reported in ref. [6], detailed comparisons of the budgets are carried out for this case only. Besides, Kasagi *et al.* [6] show that there is very little difference in the near-wall budgets of the heat fluxes for both boundary conditions. Finally, the present calculations are also compared with the model predictions of refs. [21, 23].

Since the velocity field properties have already been validated against simulation data [16, 20], the calculated properties compared here are limited to Θ^+, θ^+_{rms}, $\overline{v\theta}^+$, $\overline{u\theta}^+$, ε_θ^+, Pr_t, and the budgets of heat fluxes, temperature variance and its dissipation rate. All properties are plotted vs y^+. From (1) and (13), the following expressions can be derived for θ^+_{rms}, $\overline{v\theta}^+$, $\overline{u\theta}^+$, ε_θ^+ and $\overline{uv}^+$. They are:

$$\theta^+_{rms} = a_\theta y^+ + b_\theta y^{+2} + \cdots \quad (29a)$$

$$\varepsilon_\theta^+ = a_{\varepsilon\theta} + b_{\varepsilon\theta} y^+ + \cdots \quad (29b)$$

$$\overline{v\theta}^+ = a_{v\theta} y^{+3} + b_{v\theta} y^{+4} + \cdots \quad (29c)$$

$$\overline{u\theta}^+ = a_{u\theta} y^{+2} + b_{u\theta} y^{+3} + \cdots \quad (29d)$$

$$\overline{uv}^+ = a_{uv} y^{+3} + b_{uv} y^{+4} + \cdots. \quad (29e)$$

If these quantities are plotted in a log–log form, the slope of (29a) is 1, that of (29c) is 3 and that of (29d) is 2, while the intercepts at $\log y^+ = 0$ are a_θ, $a_{v\theta}$ and $a_{u\theta}$, respectively. The value of a_θ determined from ref. [6] is 0.262; however, no reliable values of $a_{v\theta}$ and $a_{u\theta}$ can be deduced from ref. [6]. On the other hand, the values of a_θ, $a_{v\theta}$ and $a_{u\theta}$ are quoted by Antonia and Kim [34] as 0.255, 4.795×10^{-4} and 8.642×10^{-2}, respectively, for the constant wall temperature case [3, 4]. Furthermore, from (1) and (13), it can be deduced that $a_{\varepsilon\theta} = (a_\theta)^2/Pr$. In other words, $(\theta^+_{rms})^2/\varepsilon_\theta^+ y^{+2} = Pr$ identically. These limiting values can be used to assess the asymptotic behavior and internal consistency of the near-wall two-equation model for heat fluxes.

The results for the constant wall heat flux case are presented in Figs. 1–7. Mean temperature profiles are plotted in Fig. 1(a). In the viscous sublayer, all calculated profiles agree well with the theoretical distribution, $\Theta^+ = Pr\,y^+$. The agreement extends to $y^+ = 6$; a result that is identical to the behavior shown in the simulation data [6]. Also, according to ref. [6], the von Karman constant for this flow is $\kappa_\theta = 0.36$ determined in the range, $35 < y^+ < 100$. The von Karman constants determined in the same y^+ range for the three models tested are 0.34 for ref. [21], 0.32 for ref. [23] and 0.47 for the present model. On the other hand, the effect of A^+ on the calculated mean temperature profile can be assessed by carrying out another calculation assuming $A^+ = 38$. This result is also plotted in Fig. 1(a) for comparison. From this calculation, $\kappa_\theta = 0.40$ is obtained. The underprediction of κ_θ in the case of the models of refs. [21,

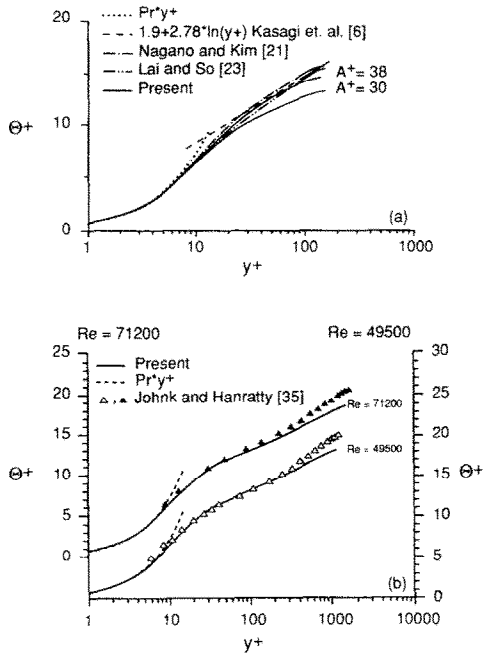

FIG. 1. Mean temperature comparison in semi-log plot for the constant wall heat flux case: (a) channel flow; (b) pipe flow.

23] is similar to the under-prediction of κ, the von Karman constant for the mean velocity profile. According to ref. [16], Lai and So's [20] prediction of κ for the channel flows of refs. [1, 2] is 0.35 compared to a direct simulation value of 0.4. It seems that the constants in these models are not optimized to adequately reflect Reynolds number effects on mean flow behavior. The present calculations adopt the model constants specified by Nagano and Kim [21] but attempt to improve the near-wall modeled behavior. This modification gives rise to a much larger value for κ_θ. However, as will be seen later, the modification improves the near-wall predictions significantly and for the first time gives a model that is asymptotically correct as a wall is approached. Furthermore, $A^+ = 30$ yields good results for high-Reynolds-number flows. This is evident in the calculations of fully-developed pipe flow heat transfer with constant wall heat flux at different Reynolds numbers, Re, which is defined in terms of pipe diameter and bulk mean velocity. The calculations are compared with measurements obtained at Re ranging from 17 700 to 71 200 [35]; however, only the results for $Re = 49\,500$ and 71 200 are plotted in Fig. 1(b). Other comparisons are not shown because they display equal or better agreement with data for the Re range of 17 700–49 500. Measurements yield a von Karman constant that varies with Re. The calculated κ_θ is in excellent agreement with data, as shown by all calculations carried out and the comparisons shown in Fig. 1(b). In other words, the Reynolds number dependence of κ_θ for the high Reynolds number range

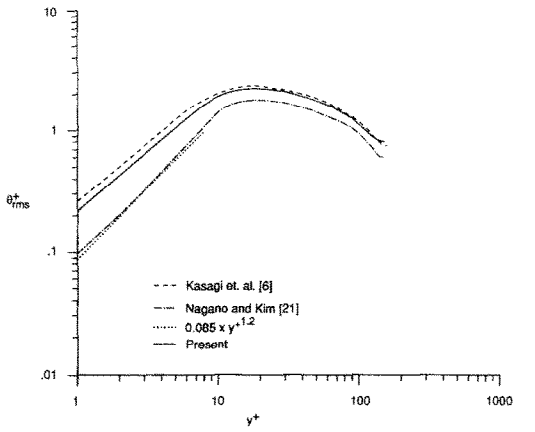

FIG. 2. Comparison of root mean square temperature variance for the constant wall heat flux case.

is correctly predicted. If $A^+ = 38$ is specified, the calculated results are not in good agreement with measurements. This, together with the fact that $A^+ = 38$, would give rise to relatively poorer near-wall predictions and suggests that the correct constant to specify for A^+ is 30, in spite of an incorrect prediction of κ_θ at $Re = 4560$.

The plots of θ^+_{rms}, $\overline{v\theta}^+$ and $\overline{u\theta}^+$ are given in Figs. 2–4. In Fig. 2, only two model calculations are shown; the present model and that of ref. [21]; while in Fig. 4, comparison is made with the model of ref. [23] only because the two-equation models cannot be used to calculate $\overline{u\theta}^+$ accurately. Therefore, their results are not compared with data. The plots of θ^+_{rms} and $\overline{v\theta}^+$ are given in log–log form so that the slopes of their variations with y^+ in the near-wall region can be determined with accuracy. It can be seen that the present model gives a slope of 1 for θ^+_{rms} (Fig. 2) and 3 for $\overline{v\theta}^+$ (Fig. 3) which are in good agreement with simulation data. On the other hand, the slopes determined from Nagano and Kim's model are 1.2 and 5 for θ^+_{rms} and $\overline{v\theta}^+$, respectively. The present model yields $a_\theta = 0.213$ and $a_{v\theta} = 4.194 \times 10^{-4}$, while the corresponding values determined from Nagano and Kim's model are 0.095 and 5.002×10^{-6}, respectively.

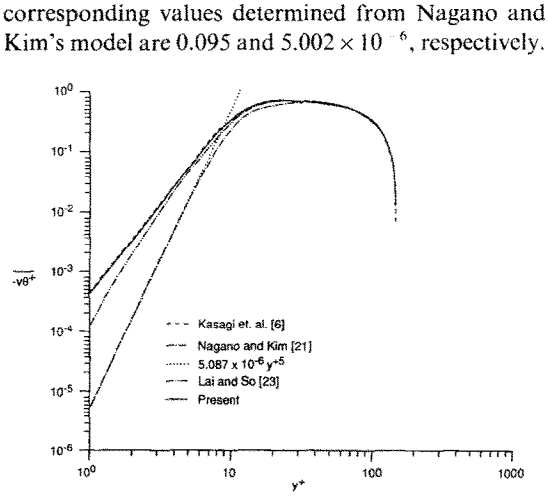

FIG. 3. Comparison of normal heat flux for the constant wall heat flux case.

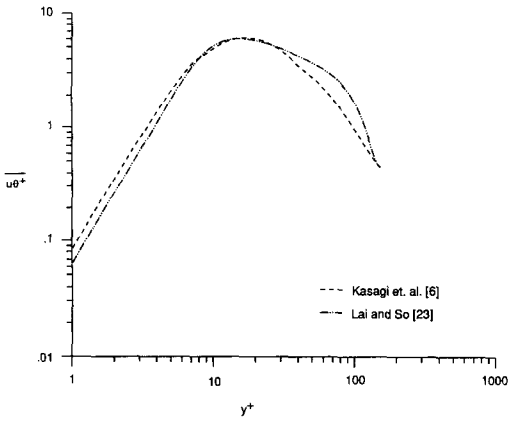

FIG. 4. Comparison of stream component heat flux for the constant wall heat flux case.

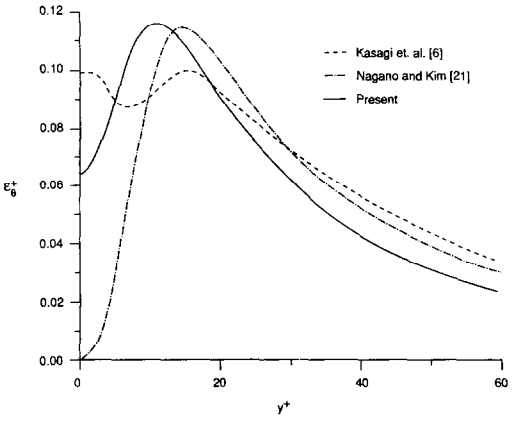

FIG. 5. Comparison of the dissipation rate of temperature variance for the constant wall heat flux case.

On the other hand, the simulation result gives a_θ as 0.262. Therefore, these results show that the near-wall model of ref. [21] fails to reproduce the correct asymptotic behavior and is incorrect in its predictions of the limiting values for $\theta^+_{\rm rms}$ and $\overline{v\theta^+}$. The $a_{v\theta}$ calculated by the model of ref. [23] is 2.687×10^{-4} and is about half that given by the present model. On the other hand, its predicted $u\theta^+$ distribution agrees well with data, in particular the behavior near the wall (Fig. 4). Again, a slope of 2 is obtained for $\overline{u\theta^+}$ at the wall; however, the calculated $a_{u\theta}$ is smaller than the simulated value (Fig. 4).

It should be pointed out that Nagano *et al.* [36]† have recently improved the model of Nagano and Kim [21] so that the predicted near-wall behavior is consistent with direct simulation data and experimental measurements. Their approach is different from that of ref. [21] and the present method in that a near-wall function $\xi_{\varepsilon\theta}$ is not proposed for (19); rather damping functions are introduced into the dissipation terms with $C_{\rm d4}$ and $C_{\rm d5}$ as coefficients to ensure proper near-wall behavior of the ε_θ equation. They further propose to model the near-wall turbulence behavior correctly for both constant wall heat flux and constant wall temperature boundary conditions. This can be accomplished by defining α_t with exponents for the velocity and thermal time scales different from those given in (20). These exponents are determined by requiring the respective boundary conditions to be properly satisfied by the model. Their results give a near-wall behavior of $\overline{v\theta^+}$ proportional to y^{+2} for the constant wall heat flux boundary condition and y^{+3} for the constant wall temperature boundary condition. The corresponding behavior for $\theta^+_{\rm rms}$ is constant and y^+, respectively. Good comparisons of mean properties are obtained with boundary-layer flows at fairly high Reynolds number; however, there are no data available to verify the near-wall behavior of the constant wall heat flux case. Even though the present model assumes the fluctuating temperature to vanish at the wall for the constant wall heat flux boundary condition, its calculated near-wall behavior of $\theta^+_{\rm rms}$ (Fig. 2) and $\overline{v\theta^+}$ (Fig. 3) is in good agreement with simulation data [6] but is not consistent with that predicted by Nagano *et al.* [36]. Therefore, further verifications with a wider range of data are required in order to establish the relative merits of each approach.

Calculated distributions of ε^+_θ are shown in Fig. 5. The model of ref. [21] yields a distribution of ε^+_θ that goes to zero at the wall. This is a consequence of the boundary condition imposed by the model. The present prediction is not in good agreement with data; however, it yields a finite ε^+_θ value at the wall. This wall value is given by $\varepsilon^+_\theta = a_{\varepsilon\theta} = 0.0639$ (Fig. 5). Therefore, based on the calculated a_θ and $a_{\varepsilon\theta}$, the limiting value of $(\theta^+_{\rm rms})^2/\varepsilon^+_\theta y^{+2}$ is determined to be 0.71, a value identically equal to the assumed Pr. A similar result can also be deduced from the model of Nagano *et al.* [36]. It is difficult to determine $a_{\varepsilon\theta}$ from ref. [6]. However, if the assumption is made that the direct simulation data do indeed yield $(\theta^+_{\rm rms})^2/\varepsilon^+_\theta y^{+2} = 0.71$, the assumed Pr, then $a_{\varepsilon\theta}$ is calculated to be 0.097. The present model yields a value of 0.0639 for $a_{\varepsilon\theta}$ (Fig. 5) and is substantially lower than the simulation value. According to the model of ref. [21], $a_{\varepsilon\theta} = 0$; therefore, its prediction of $(\theta^+_{\rm rms})^2/\varepsilon^+_\theta y^{+2}$ at the wall is infinite. This suggests that the model of ref. [21] is asymptotically incorrect.

The budgets of temperature variance and its dissipation rate are shown in Figs. 6 and 7, respectively. Only the calculations from the present model and that of ref. [21] are compared in these figures. These two model calculations cannot provide budgets for the heat fluxes because their transport equations are not solved. On the other hand, the heat flux model provides budgets for the heat fluxes and they have been analysed in ref. [23]. Therefore, their presentations are not repeated here. In general, the present model

† The authors are grateful to one of the referees who brought this recent paper of Nagano *et al.* [36] to our attention. We would like to thank the referee for his critical review of our paper.

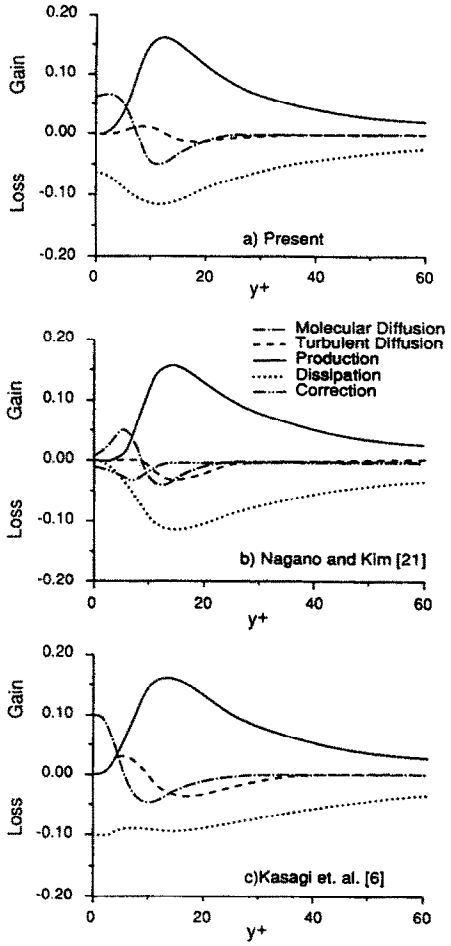

FIG. 6. Comparison of the budget of temperature variance for the constant wall heat flux case: (a) present model calculation; (b) Nagano and Kim's model [21] calculation; (c) direct simulation data [6].

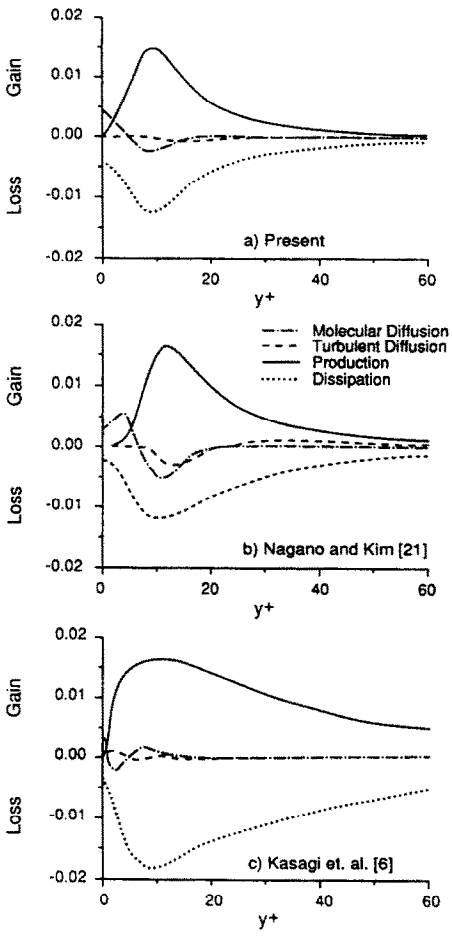

FIG. 7. Comparison of the budget of the dissipation rate of temperature variance for the constant wall heat flux case: (a) present model calculation; (b) Nagano and Kim's model [21] calculation; (c) direct simulation data [6].

gives a better prediction of the budgets of $\overline{\theta^2}/2$ and ε_θ, including the correct prediction of the maximum production of $\overline{\theta^2}/2$ and its location and the behavior of molecular diffusion in the region $0 < y^+ < 25$.

The results for the constant wall temperature case are shown in Figs. 8–11. Again, the simulation data yield a von Karman constant $\kappa_\theta = 0.36$. The calculated profiles in the sublayer agree with $\Theta^+ = Pr\, y^+$ up to $y^+ = 6$ (Fig. 8). However, the calculated κ_θ is 0.37 for the model of ref. [21], 0.35 for the model of ref. [23] and 0.50 for the present model with $A^+ = 30$. If $A^+ = 38$ is assumed, the calculated profile yields $\kappa_\theta = 0.45$, which is in better agreement with data compared to the $A^+ = 30$ result (Fig. 8). The higher prediction of κ_θ for this case could be due to the fact that the model constants have not been properly optimized for low-Reynolds-number flows.

The near-wall behavior of the thermal field is reproduced correctly by the present model as shown by the comparisons of $\theta^+_{\rm rms}$, $\overline{v\theta^+}$ and $\overline{u\theta^+}$ in Figs. 9–11. In a log–log plot, the slopes of $\theta^+_{\rm rms}$ and $\overline{v\theta^+}$ vs y^+ are determined to be 1 (Fig. 9) and 3 (Fig. 10), respectively, and are in good agrement with simulation data. The corresponding slopes calculated from the model of ref. [21] are 1.2 and 5. As for a_θ and $a_{v\theta}$, the values

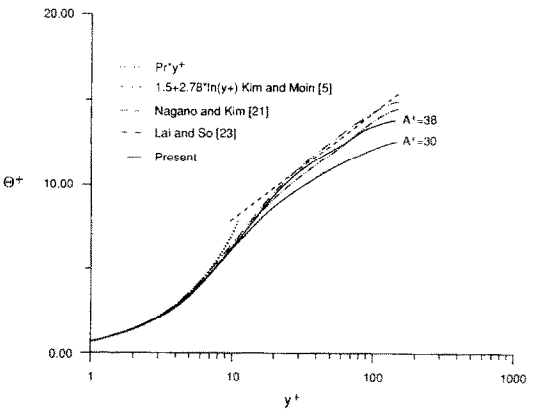

FIG. 8. Mean temperature comparison in semi-log plot for the constant wall temperature case.

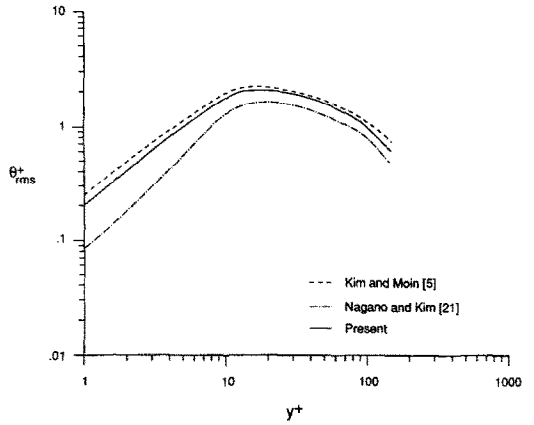

FIG. 9. Comparison of root mean square temperature variance for the constant wall temperature case.

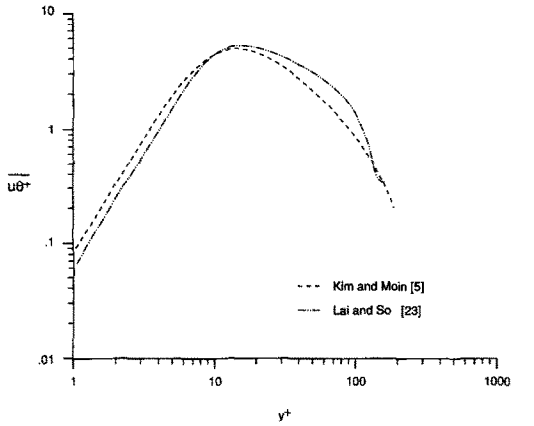

FIG. 11. Comparison of stream component heat flux for the constant wall temperature case.

predicted by the present model are 0.203 and 4.177×10^{-4}, respectively, while the corresponding values obtained from the model of ref. [21] are 0.086 and 4.816×10^{-6}. These compare with values of 0.255 and 4.795×10^{-4} reported by Antonia and Kim [34] for the data of refs. [4, 5]. In view of these comparisons it can be said that the model of ref. [21] is also asymptotically incorrect for the constant wall temperature boundary condition. The values of $(\theta^+_{rms})^2/\varepsilon^+_\theta y^{+2}$ and $a_{\varepsilon\theta}$ are not reported in refs. [4, 5, 32]. If it is assumed that $(\theta^+_{rms})^2/\varepsilon^+_\theta y^{+2}$ is again given by 0.71, then $a_{\varepsilon\theta}$ can be determined to be 0.092 for the direct simulation data of refs. [4, 5]. As before, the present model under-predicts $a_{\varepsilon\theta}$, which is calculated to be 0.058 (Fig. 10), but its prediction of $(\theta^+_{rms})^2/\varepsilon^+_\theta y^{+2}$ is still 0.71. These results are in excellent agreement with Nagano *et al.*'s [36] predictions, which yield values of 0.054 and 0.71, respectively. Prediction of $\overline{u\theta^+}$ by the model of ref. [23] compares favorably with simulation data (Fig. 11). The slope is calculated to be 2 and $a_{u\theta}$ is determined as 6.1×10^{-2}, which is smaller than the simulation value of 8.642×10^{-2}. The calculated distributions of ε^+_θ are similar to the constant wall heat flux case and the model of ref. [21] again gives a zero wall value for ε^+_θ, contrary to

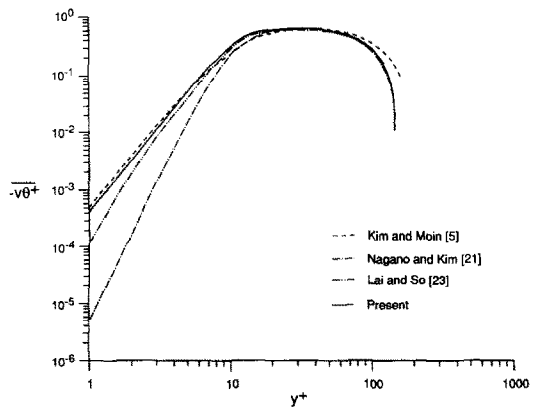

FIG. 10. Comparison of normal heat flux for the constant wall temperature case.

simulation data and present prediction. Once again, these comparisons indicate that the present model and that of ref. [23] behave correctly as a wall is approached.

According to Antonia and Kim [34], who analyse the simulation data of refs. [4, 5] for their asymptotic near-wall behavior, Pr_t at the wall is determined to be approximately 1.1. Since Pr_t at the wall is given by

$$Pr_t = \frac{\overline{uv^+}\,(\partial\Theta^+/\partial y^+)}{\overline{v\theta^+}\,(\partial U^+/\partial y^+)} = \frac{a_{uv}\,Pr}{a_{v\theta}} \tag{30}$$

the correct prediction of Pr_t depends on the calculated values of a_{uv} and $a_{v\theta}$. The present model gives $a_{uv} = 0.20 \times 10^{-3}$ and $a_{v\theta} = 0.418 \times 10^{-3}$, while the heat flux model yields $a_{uv} = 0.20 \times 10^{-3}$ and $a_{v\theta} = 0.25 \times 10^{-3}$ and the model of ref. [21] predicts $a_{v\theta} = 0.482 \times 10^{-5}$. On the other hand, according to ref. [34], simulation data give $a_{uv} = 0.748 \times 10^{-3}$ and $a_{v\theta} = 0.479 \times 10^{-3}$. It can be seen that the present model predicts $a_{v\theta}$ with fair accuracy but is in error by a factor of 3.7 in the prediction of a_{uv}. The model of ref. [23] predicts $a_{v\theta}$ to be about half that of the simulation data. Consequently, the wall values of Pr_t predicted by these two models are 0.34 and 0.57, respectively. On the other hand, the model of ref. [21] yields an $a_{v\theta}$ that is two orders of magnitude smaller. If the same a_{uv} is assumed, then the model of ref. [21] yields a Pr_t at the wall equal to 0.29×10^2, which is two orders of magnitude larger than simulation data. Since a_{uv} and $a_{v\theta}$ are very small, numerical errors involved in their calculations are large. Consequently, numerical accuracy as well as near-wall modeling has an important effect on the prediction of Pr_t at the wall.

CONCLUSIONS

A near-wall two-equation model for heat fluxes has been derived. The model is based on the transport equations for temperature variance and its dissipation rate. It is derived by modifying a conventional two-equation model for high-Reynolds-number flows and

by invoking a gradient transport assumption for the heat fluxes. All constants in the modeled high-Reynolds-number equations are adopted without change. Consequently, the near-wall modeled equations reduce exactly to the high-Reynolds-number equations away from a wall. The near-wall corrections are deduced by analyzing the terms in the exact equations and in the high-Reynolds-number modeled temperature variance and its dissipation rate equations. Near-wall imbalances of the different terms in these equations are evaluated and proposals are made to remedy the imbalance, at least up to first order of the normal coordinate. An eddy conductivity is proposed to relate turbulent heat fluxes to the mean temperature field. The proposed eddy conductivity involves both velocity and thermal time scales and behaves correctly near a wall. Therefore, the modeled normal heat flux approaches the wall in a manner identical to that of the exact behavior. A recently developed near-wall Reynolds-stress model is selected for use with the near-wall two-equation model to calculate fully-developed pipe and channel flows with constant wall heat flux and constant wall temperature boundary conditions. The calculations of these two cases are compared with direct simulation data [4–6] and with the predictions of the near-wall two-equation model of ref. [21] and the near-wall heat flux model of ref. [23].

Results show that the present model is deficient in its predictions of mean temperature for the two low-Reynolds-number cases considered. It over-predicts the value of κ_θ substantially. However, the models of refs. [21, 23] calculate κ_θ with fair accuracy for both cases. This discrepancy can be traced to the model constants used which, strictly speaking, are tuned for high-Reynolds-number flows. On the other hand, all three models tested give a correct prediction of the temperature profile in the viscous sublayer. As for the turbulence statistics, the present model and the model of ref. [23] yield correct asymptotic behavior at the wall for the temperature variance and its dissipation rate and the heat fluxes, and provide a fairly good estimate of their limiting wall values. In addition, the present model correctly predicts $(\theta^+_{\rm rms})^2/\varepsilon^+_\theta y^{+2} = 0.71$, the assumed Pr, while the model of ref. [21] yields an infinite value for this parameter. In view of this, it can be concluded that the present model is internally consistent and asymptotically correct as a wall is approached but the model of ref. [21] is not.

Acknowledgement—The authors wish to acknowledge the support given them by NASA Langley Research Center, Hampton, Virginia, under Grant No. NAG-1-1080 monitored by Dr T. B. Gatski.

REFERENCES

1. J. Kim, P. Moin and R. D. Moser, Turbulence statistics in fully developed channel flow at low Reynolds number, *J. Fluid Mech.* **177,** 133–186 (1987).
2. N. N. Mansour, J. Kim and P. Moin, Reynolds-stress and dissipation-rate budgets in a turbulent channel flow, *J. Fluid Mech.* **194,** 15–44 (1988).
3. P. R. Spalart, Direct simulation of a turbulent boundary layer up to $R_\theta = 1410$, *J. Fluid Mech.* **187,** 61–98 (1988).
4. J. Kim, Investigation of heat and momentum transport in turbulent flows via numerical simulations. In *Transport Phenomena in Turbulent Flows* (Edited by M. Hirata and N. Kasagi), pp. 715–730. Hemisphere, New York (1988).
5. J. Kim and P. Moin, Transport of passive scalars in a turbulent channel flow. In *Turbulent Shear Flows 6*, pp. 85–96. Springer, Berlin (1989).
6. N. Kasagi, Y. Tomita and A. Kuroda, Direct numerical simulation of the passive scalar field in a two-dimensional turbulent channel flow, *3rd ASME–JSME Thermal Engineering Joint Conf.*, Reno (March 1991).
7. Y. Iritani, N. Kasagi and M. Hirata, Heat transfer mechanism and associated turbulence structure in the near-wall region of a turbulent boundary layer. In *Turbulent Shear Flows 4*, pp. 223–234. Springer, Berlin (1985).
8. M. Hishida, Y. Nagano and M. Tagawa, Transport processes of heat and momentum in the wall region of turbulent pipe flow, *Proc. Eighth Int. Heat Transfer Conf.*, Vol. 3, pp. 925–930 (1986).
9. L. V. Krishnamoorthy and R. A. Antonia, Temperature dissipation measurements in a turbulent boundary layer, *J. Fluid Mech.* **176,** 265–281 (1987).
10. L. V. Krishnamoorthy and R. A. Antonia, Turbulent kinetic energy budget in the near-wall region, *AIAA J.* **26,** 300–302 (1987).
11. V. C. Patel, W. Rodi and G. Scheuerer, Turbulence models for near-wall and low-Reynolds-number flows: a review, *AIAA J.* **23,** 1308–1319 (1985).
12. Y. Nagano and M. Hishida, Improved form of the k–ε model for wall turbulent shear flows, *J. Fluids Engng* **109,** 156–160 (1987).
13. K. Hanjalic and B. E. Launder, Contribution towards a Reynolds-stress closure for low-Reynolds-number turbulence, *J. Fluid Mech.* **74,** 593–610 (1976).
14. R. M. C. So and G. J. Yoo, Low-Reynolds-number modelling of turbulent flows with and without wall transpiration, *AIAA J.* **25,** 1556–1564 (1987).
15. R. M. C. So, H. S. Zhang and C. G. Speziale, Near-wall modeling of the dissipation-rate equation, *AIAA J.* **29,** 2069–2076 (1991).
16. R. M. C. So, Y. G. Lai, H. S. Zhang and B. C. Hwang, Second-order near-wall turbulence closures: a review, *AIAA J.* **29,** 1819–1835 (1991); also NASA Contractor Report 4369 (1991).
17. H. K. Myong and N. Kasagi, A new approach to the improvement of the k–ε turbulence model for wall bounded shear flows, *JSME Int. J. Ser. II* **33,** 63–72 (1990).
18. N. Shima, A Reynolds-stress model for near-wall and low-Reynolds-number regions, *J. Fluids Engng* **110,** 38–44 (1988).
19. B. E. Launder and N. Shima, Second-moment closure for the near-wall sublayer: development and application, *AIAA J.* **27,** 1319–1325 (1989).
20. Y. G. Lai and R. M. C. So, On near-wall turbulent flow modeling, *J. Fluid Mech.* **221,** 641–673 (1990).
21. Y. Nagano and C. Kim, A two-equation model for heat transport in wall turbulent shear flows, *J. Heat Transfer* **110,** 583–589 (1988).
22. H. K. Myong, N. Kasagi and M. Hirata, Numerical prediction of turbulent pipe flow heat transfer for various Prandtl number fluids with the improved k–ε turbulence model, *JSME Int. J. Ser. II* **32,** 613–623 (1989).
23. Y. G. Lai and R. M. C. So, Near-wall modeling of turbulent heat fluxes, *Int. J. Heat Mass Transfer* **33,** 1429–1440 (1990).

24. B. E. Launder, Heat and mass transport, *Turbulence—Topics in Applied Physics* (Edited by P. Bradshaw), pp. 232–287. Springer, Berlin (1976).
25. B. E. Launder, On the computation of convective heat transfer in complex turbulent flows, *J. Heat Transfer* **110,** 1112–1128 (1988).
26. W. P. Jones and P. Musonge, Closure of the Reynolds-stress and scalar flux equations, *Phys. Fluids* **31,** 3589–3604 (1988).
27. G. R. Newman, B. E. Launder and J. L. Lumley, Modelling of the behavior of homogeneous scalar turbulence, *J. Fluid Mech.* **111,** 217–232 (1981).
28. S. E. Elghobashi and B. E. Launder, Turbulent time scales and the dissipation ratio of temperature variance in the thermal mixing layer, *Phys. Fluids* **26,** 2415–2419 (1983).
29. A. Yoshizawa, Statistical modelling of passive-scalar diffusion in turbulent shear flows, *J. Fluid Mech.* **195,** 541–555 (1988).
30. A. F. Polyakov, Wall effect on temperature fluctuations in the viscous sublayer, *Teplofizika Vysokikh Temperatur* **12,** 328–337 (1974).
31. S. E. Elghobashi and J. C. LaRue, The effect of mechanical stream on the dissipation rate of a scalar variance, *Proc. 4th Symp. on Turbulent Shear Flows*, Karlesruhe, Germany, pp. 1–5 (1983).
32. N. Kasagi and K. Nishiro, Probing turbulence with three-dimensional particle tracking velocimetry. In *Engineering Turbulence Modelling and Experiments* (Edited by W. Rodi and E. N. Ganic), pp. 299–314. Elsevier, New York (1990).
33. B. E. Launder, G. J. Reece and W. Rodi, Progress in the development of a Reynolds stress turbulence closure, *J. Fluid Mech.* **68,** 537–566 (1975).
34. R. A. Antonia and J. Kim, Turbulent Prandtl number in the near-wall region of a turbulent channel flow, *Int. J. Heat Mass Transfer* **34,** 1905–1908 (1991).
35. R. E. Johnk and T. J. Hanratty, Temperature profiles for turbulent flow of air in a pipe—I. The fully developed heat transfer region, *Chem. Engng Sci.* **17,** 867–879 (1962).
36. Y. Nagano, M. Tagawa and T. Tsuji, An improved two-equation heat transfer model for wall turbulent shear flows, *ASME/JSME Thermal Engineering Proc.*, Vol. 3, pp. 233–240 (1991).